JOURNAL OF PHYSICAL ORGANIC CHEMISTRY, VOL. 5, 507–517 (1992)

HOST–GUEST CHEMISTRY. METHANOL, ETHANOL AND PROPAN-1-OL INCLUSION COMPOUNDS OF 2-[*o*-(TRIPHENYLPHOSPHORANYLIDENAMINO) BENZYLIDEN]AMINO-1*H*-2,3-DIHYDROINDAZOL-3-ONE. X-RAY STRUCTURAL CHARACTERIZATION OF THE FREE HOST AND ITS ETHANOL INCLUSION COMPOUND

PEDRO MOLINA,* ANTONIO ARQUES AND ROSARIO OBÓN

Departamento de Química Orgánica, Facultad de Ciencias, Universidad de Murcia, Campus de Espinardo, 30071 Murcia, Spain

ANTONIO L. LLAMAS-SAIZ AND CONCEPCION FOCES-FOCES*

UEI de Cristalografía, Instituto de Química Física 'Rocasolano,' CSIC, Serrano 119, 28006 Madrid, Spain

AND

ROSA MARIA CLARAMUNT,* CONCEPCION LÓPEZ AND JOSE ELGUERO

Departamento de Química Orgánica y Biología, Facultad de Ciencias, UNED, Ciudad Universitaria, 28040 Madrid, Spain

The title compound (3) which is a 2-aminoindazol-3-one derivative linked through a methinephenyl bridge to an iminophosphorane, and unrelated to any previous host, is described. The bulky triphenylphosphino group provides the cavity and the indazol-3-one the hydrogen bonds (both donor —NH— and acceptor —CO—). X-ray structural analyses of the free host 3 and that of its ethanol inclusion compound 3 · EtOH are reported. Hydrogen bonds resulting in infinite chains dominate the molecular packing. The use of thermal analysis and ^{13}C CP/MAS NMR shed light in the structures of two other inclusion compounds, 3 · MeOH and 3 · PrOH. The conclusion is that all three compounds are similar. An analysis of the cavities, using a model of interpenetrating spheres of van der Waals radii, demonstrates that in the case of the ethanol derivative, the cavity has the space and form requirements necessary to include the propanol guest.

INTRODUCTION

In recent years we have become involved in host–guest chemistry with particular emphasis on the X-ray structural determination of inclusion compounds.[1–7] One of the aims of that research was to find new hosts and to study the form[8] and size[9] of the cavities before and after the guest is inside it. In this paper, we describe a new host, the title compound **3** with a structure related both to iminophosphoranes[5] and to indazolones.[10]

Recently, the iminophosphorane **2** has been prepared by the Staudinger reaction between *o*-azidobenzaldehyde **1** and triphenylphosphine (TPP) in toluene at room temperature.[11] In our hands, the reaction of *o*-azidobenzaldehyde with TPP in dry dichloromethane at 0 °C followed by chromatographic separation (silica gel and ethyl acetate–hexane as eluent) and crystallization gave *o*-(triphenylphosphoranyliden)aminobenzaldehyde **2** (30%) and the iminophosphorane **3** (25%). However, when the reaction was carried out in diethyl ether −20 °C, the phosphazide **4** was isolated as the only reaction product.

A tentative mechanism for the conversion **1** → **2** + **3** is represented in Scheme 1. It involves the initial formation of the phosphazide **4**, which after nitrogen evolution leads to **2**. Alternatively, the phosphazide **4** undergoes a [1, 5] proton shift to give **5**, which cyclizes by nucleophilic attack of the amino group on the

* Authors for correspondence.

0894–3230/92/080507–11$10.05

Received 4 February 1992
Revised 14 April 1992

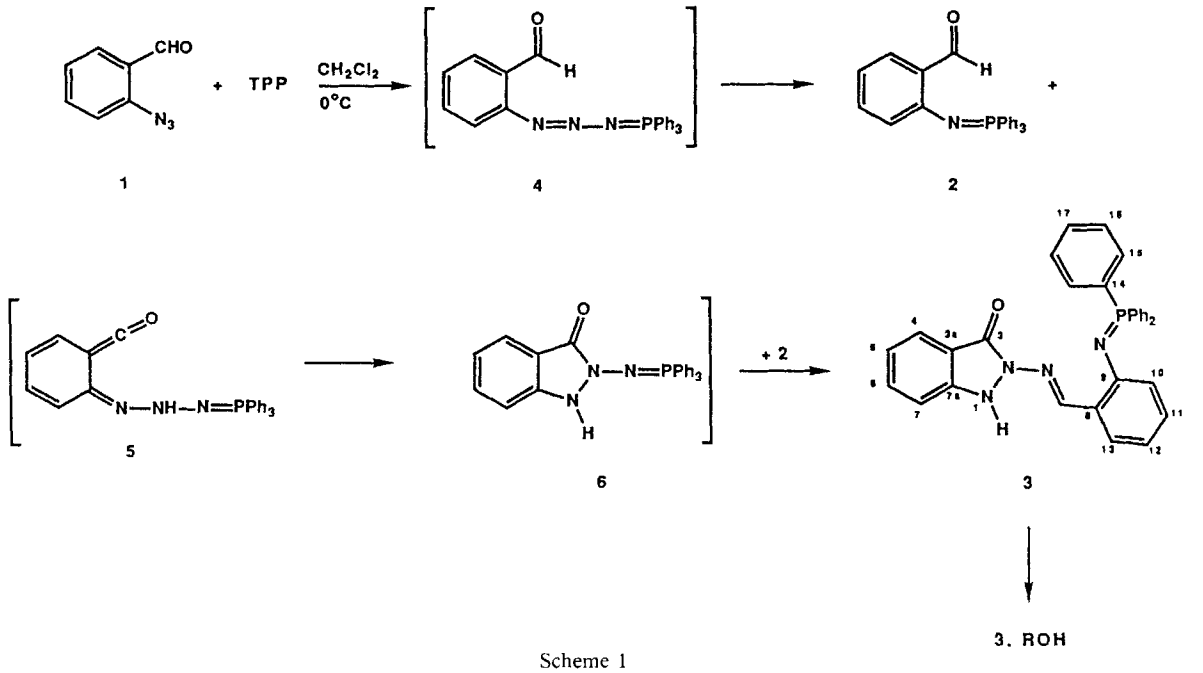

Scheme 1

central carbon atom of the ketene moiety to give **6**. Finally, an intermolecular aza-Wittig reaction between **2** and **6** leads to **3**.

EXPERIMENTAL

Melting points were determined with a Kofler hot-stage microscope and are uncorrected. Spectral studies were performed with the following instruments: NMR (see later); IR, Nicolet FT-5DX; MS (70 eV), Hewlett-Packard 5993C. Combustion analyses were performed with a Perkin-Elmer 240C instrument.

Preparation of the host **3**. To a solution of triphenylphosphine (1·78 g, 6·7 mmol) in dry dichloromethane (10 ml) at 0 °C, a solution of *o*-azidobenzaldehyde **1** (1·0 g, 6·7 mmol) in the same solvent (20 ml) was added dropwise under nitrogen and the reaction mixture was stirred at room temperature for 16 h. The solvent was removed under reduced pressure and the residual material was chromatographed on a silica gel column, eluting with ethyl acetate–hexane (3 : 1) to afford the iminophosphorane **2** derived from *o*-azidobenzaldehyde (0·7 g, 30%; m.p. 175 °C, lit.[12] m.p. 173–174 °C) and **3** (0·87 g, 25%; m.p. 185 °C) as yellow crystals.

Analysis for $C_{32}H_{25}N_4PO$ (512·55): calculated, C 74·99, H 4·92, N 10·93; found, C 75·18, H 4·98, N 11·05%. ^{1}H NMR (200 MHz): 7·86 (H-4, $^3J_{4,5}$ = 7·8 Hz), 7·15 (H-5, $^3J_{5,6}$ = 7·2 Hz), 7·01 (H-7, $^3J_{6,7}$ = 8·1 Hz), 9·46 (N=CH), 6·49 (H-10, $^3J_{10,11}$ = 8·1 Hz), 6·93 (H-11, $^3J_{11,12}$ = 7·2 Hz, $^4J_{11,13}$ = 1·8 Hz), 6·71 (H-12, $^3J_{12,13}$ = 7·8 Hz), 7·92 (H-13), 7·58 (H-15, $^3J_{15^{31}P}$ = 12.1 Hz, $^3J_{15,16}$ = 7·6 Hz, $^4J_{15,17}$ = 1·4 Hz), 7·30–7·50 (m, 17H, H-6, NH, H-16, H-17). ^{13}C NMR (50 MHz, the reported couplings refer to ^{13}C–^{31}P): 159·12 (C-3), 119·36 (C-3a), 124·16 (C-4), 122·40 (C-5), 132·45 (C-6), 113·04 (C-7), 145·76 (C-7a) (this assignment is consistent with that of 2-methylindazolone),[10] 145·85 (N=CH), 127·96 (C-8, ^3J = 17·8), 155·55 (C-9, ^2J = 1·8), 123·08 (C-10, ^3J = 9·2), 130·60 (C-11), 118·74 (C-12), 127·31 (C-13), 129·79 (C-14, ^1J = 99·6 Hz), 132·55 (C-15, ^2J = 9.8), 128·70 (C-16, ^3J = 12·2), 132·02 (C-17, ^4J = 2·8 Hz). Mass spectrum (Th, %): 512 (M^+, 5), 134 (100). IR (Nujol): 1642 cm^{-1}.

Preparation of inclusion compounds **3** · *ROH*. A suspension of **3** (0·5 g, 97·6 mmol) in the appropriate alcohol (20 ml) was stirred at room temperature for 7 h. The separated solid was collected by filtration, washed with diethyl ether, air dried and recrystallized from the same alcohol.

3 · *MeOH*. Yield 0·2 g (38%), m.p. 151–152 °C. Analysis for $C_{33}H_{29}N_4PO_2$ (544·59): calculated, C 72·78, H 5·37, N 10·29; found, C 72·91, H 5·27, N 10·42%. ^{1}H NMR (200 MHz): the signals of the free host plus those of methanol at 3·42 (s, CH_3) and 5·25

(s br, OH). ^{13}C NMR (50 MHz): the signals of the free host plus that of methanol at 50·60 ppm (CH_3). Mass spectrum (Th, %): 379 (14), 377 (56), 183 (100). IR (Nujol): 1672, 1593, 1353, 1111, 754, 721, 691, 675 cm^{-1}.

3·EtOH. Yield 0·21 g (40%), m.p. 133–134 °C. Analysis for $C_{34}H_{31}N_4PO_2$ (558·62): calculated, C 73·10, H 5·59, N 10·03; Found, C 73·27, H 5·50, N 9·90%. ^1H NMR (200 MHz): the signals of the free host plus those of ethanol at 1·17 (t, CH_3, $^3J = 7·0$ Hz), 3·65 (q, CH_2) and 5·60 (s br, OH). ^{13}C NMR (50 MHz): the signals of the free host plus those of ethanol at 18·27 (CH_3) and 58·17 (CH_2). Mass spectrum (Th, %): 379 (5), 377 (19), 183 (20), 134 (100). IR (Nujol): 1676, 1352, 1231, 1112, 752, 721, 690 cm^{-1}.

3·PrOH. Yield 0·19 g (46%), m.p. 132–133 °C. Analysis for $C_{35}H_{33}N_4PO_2$ (572·65): calculated, C 73·41, H 5·81, N 9·78; found, C 73·57, H 5·90, N 9·90%. ^1H NMR (200 MHz): the signals of the free host plus those of propanol at 0·88 (t, CH_3, $^3J = 7·4$ Hz), 1·53 (m, central CH_2), 3·54 (t, CH_2OH, $^3J = 8·1$ Hz) and 4·50 (s br, OH). ^{13}C (50 MHz): the signals of the free host plus those of propanol at 10·07 (CH_3), 25·74 (central CH_2) and 64·43 (CH_2OH). Mass spectrum (Th, %): 512 (M^+ – PrOH, 1), 497 (8), 377 (30), 183 (100). IR (Nujol): 1676, 1593, 1235, 1111, 751, 721, 691 cm^{-1}.

Thermal analysis. Differential scanning calorimetric (DSC) and thermogravimetric (TG) studies were carried out under nitrogen on a Metler DSC-20 calorimeter and a Mettler TG-50 thermobalance.

X-ray crystallography. Crystal data for **3**: monoclinic, $P2_1/c$, $a = 25·2181(16)$, $b = 10·6214(3)$, $c = 21·3475(12)$ Å, $\beta = 113·082(4)°$, $V = 5260·2(5)$ Å^3, $d_c = 1·294$ g cm^{-3}, $Z = 8$, crystal dimensions $0·50 \times 0·23 \times 0·07$ mm, $\theta_{max} = 65°$, 8844 independent reflections, R (R_w) = 0·045 (0·050) for 6693 [$I > 3\sigma(I)$] observed reflections, $\mu = 11·62$ cm^{-1}.

Crystal data for **3**·EtOH: triclinic, $P\bar{1}$, $a = 21·6674(26)$, $b = 10·9789(10)$, $c = 12·6855(11)$ Å, $\alpha = 91·097(6)$, $\beta = 95·460(7)$, $\gamma = 98·780(10)°$, $V = 2967·1(5)$ Å^3, $d_c = 1·251$ g cm^{-3}, $Z = 4$, crystal dimensions $0·20 \times 0·17 \times 0·03$ mm, $\theta_{max} = 60°$, 8823 independent reflections, R (R_w) = 0·082 (0·076) for 4422 [$I > 3\sigma(I)$] observed reflections, $\mu = 10·93$ cm^{-1}.

A Philips PW1100 diffractometer was used with Cu Kα radiation and a graphite monochromator. Direct methods and refinement on F_0 were used. All hydrogen atoms were located on the corresponding difference Fourier map. Some hydrogen parameters in **3**·EtOH were kept fixed in the last cycles of the refinement. Most of the calculations were done on a Vax 6410 computer using the following set of programs: SIR88,[13] XRAY80,[14] XTAL3.0[15] and PESOS.[16] Empirical absorption corrections for all compounds were performed using the program DIFABS[17] and the scattering factors were taken from the *International Tables for X-Ray Crystallography*.[18]

NMR spectroscopy. The ^1H and ^{13}C NMR spectra in solution were obtained with a Bruker AC-200 spectrometer (University of Murcia) [all chemical shifts are expressed in ppm relative to tetramethylsilane (TMS)]. The ^{13}C data were obtained with the following conditions: number of data points, 65 536; flip angle, 30°; pulse width, 30 μs; acquisition time, 1·0 s. Solutions in DMSO-d_6 were prepared by dissolving 100 mg of sample in 1 ml of solvent. The ^{13}C NMR solid-state spectra were recorded on a Bruker AC-200 spectrometer (UNED) working at 50·32 MHz, using 3·5 kHz spinning speed and 7 mm o.d. ZrO_2 rotors. The single-constant spin-locking cross-polarization pulse sequence was used under Hartmann–Hahn conditions. The contact and repetition times were chosen to be 3 ms and 5 s, respectively. A spectral width of 20·0 kHz and 1K acquisition data points were used. Chemical shifts were measured with respect to the spectrometer reference frequency, which was calibrated with the glycine signal (176·35 ppm downfield from TMS).

RESULTS AND DISCUSSION

The results of the thermal analysis are given in Table 1. For all three compounds, the TG curves show experimental weight losses, which are in excellent agreement with calculated values (differences < 1%). The DSC curves show an endothermic peak near 120 °C, which corresponds to the weight loss in the TG curve. This is followed either by two exothermic peaks at 140–147 °C and 155–160 °C, for **3**·MeOH and **3**·EtOH, or one exothermic peak at 167 °C, for **3**·PrOH. The DSC curve of the host also shows this exothermic peak at 169 °C. Finally, the melting endotherm of the host appears at 323 °C. In all cases, the value obtained for ΔH by DSC is higher than the corresponding molar heat of vaporization.[19] Since the thermodynamic properties of the inclusion compounds can be split into contributions from the host and guest substances,[20] we can use the difference ($\delta\Delta H = \Delta H - \Delta H_v$) as a measure of the lattice cohesion. The values in Table 4 show that $\delta\Delta H$ is almost constant, indicating that all the three compounds have similar crystal structures, particularly similar hydrogen bonds between the host and the guest.

To discuss the X-ray structures, a drawing of molecule 2 of compound **3** with the atomic numbering scheme is shown in Figure 1. Table 2 gives selected bond lengths, bond angles and torsion angles.

The two independent molecules in **3**·EtOH (almost

Table 1. Results of the thermal analyses

Alcohol	Thermogravimetry: Temperature Range (°C)	Thermogravimetry: Temperature Peaks	Thermogravimetry: ΔM (%) Found	Thermogravimetry: ΔM (%) Required	Differential scanning calorimetry: DSC peaks[a] (°C)	Differential scanning calorimetry: ΔH (kcal mol^{-1})	Differential scanning calorimetry: ΔH_v^{19} (kcal mol^{-1})
MeOH	105–158	133	5·94	5·88	125	14·16	9·4
EtOH	93–151	137	8·32	8·24	120	14·00	9·7
PrOH	98–140	126	10·56	10·49	120	15·55	11·3

[a] Endothermic processes.

Table 2. Selected bond distances (Å), angles and torsion angles (°)

Compound	3		3·EtOH	
	1[a]	2[a]	1[a]	2[a]
N(*i*01)—N(*i*02)	1·428(3)	1·422(3)	1·412(10)	1·428(11)
N(*i*01)—C(*i*07A)	1·394(3)	1·396(4)	1·409(12)	1·412(11)
N(*i*02)—C(*i*03)	1·378(3)	1·377(3)	1·388(12)	1·389(11)
N(*i*02)—N(*i*09)	1·372(3)	1·364(4)	1·372(10)	1·361(9)
C(*i*03)—C(*i*03A)	1·445(4)	1·444(4)	1·441(13)	1·438(14)
C(*i*03)—O(*i*08)	1·234(3)	1·238(3)	1·221(12)	1·242(13)
N(*i*09)—C(*i*10)	1·282(3)	1·284(4)	1·300(12)	1·303(11)
C(*i*10)—C(*i*11)	1·456(3)	1·455(4)	1·446(12)	1·446(11)
C(*i*11)—C(*i*12)	1·417(3)	1·412(4)	1·405(12)	1·422(11)
C(*i*12)—N(*i*17)	1·381(4)	1·388(3)	1·373(10)	1·379(12)
N(*i*17)—P(*i*18)	1·560(2)	1·579(3)	1·568(7)	1·574(7)
O(*i*50)—C(*i*51)	—	—	1·431(15)	1·466(17)
C(*i*51)—C(*i*52)	—	—	1·410(21)	1·427(20)
C(*i*07A)—N(*i*01)—H(*i*01)	112(2)	116(2)	121(5)	115(10)
N(*i*02)—N(*i*01)—H(*i*01)	112(2)	108(2)	115(5)	109(10)
N(*i*02)—N(*i*01)—C(*i*07A)	104·0(2)	103·5(2)	102·3(6)	101·9(7)
N(*i*02)—C(*i*03)—O(*i*08)	125·2(2)	124·8(3)	124·1(9)	123·6(9)
N(*i*02)—C(*i*03)—C(*i*03A)	105·2(2)	104·5(2)	103·2(8)	105·2(8)
N(*i*02)—N(*i*09)—C(*i*10)	117·1(2)	119·1(2)	118·8(7)	117·3(7)
N(*i*09)—C(*i*10)—C(*i*11)	122·2(2)	118·8(2)	121·7(8)	118·8(8)
C(*i*10)—C(*i*11)—C(*i*16)	122·0(2)	119·0(2)	120·8(8)	124·0(8)
C(*i*10)—C(*i*11)—C(*i*12)	118·5(2)	120·9(2)	118·3(7)	117·6(7)
C(*i*11)—C(*i*12)—N(*i*17)	117·7(2)	119·0(2)	117·9(7)	116·5(7)
C(*i*13)—C(*i*12)—N(*i*17)	124·6(3)	124·5(2)	125·1(7)	124·8(8)
C(*i*12)—N(*i*17)—P(*i*18)	134·4(2)	126·4(2)	130·5(6)	132·2(6)
O(*i*50)—C(*i*51)—C(*i*52)	—	—	111·3(11)	110·4(13)
N(*i*02)—N(*i*01)—C(*i*07A)—C(*i*03A)	−5·6(3)	−7·1(3)	4·5(10)	5·2(10)
C(*i*07A)—N(*i*01)—N(*i*02)—C(*i*03)	6·1(3)	8·9(3)	−5·1(9)	−6·4(9)
N(*i*01)—N(*i*02)—N(*i*09)—C(*i*10)	6·7(3)	4·3(4)	−7·9(12)	−9·3(11)
N(*i*01)—N(*i*02)—C(*i*03)—C(*i*03A)	−4·1(3)	−7·2(3)	3·7(10)	5·3(10)
N(*i*02)—C(*i*03)—C(*i*03A)—C(*i*07A)	0·5(3)	2·5(3)	−0·7(10)	−1·8(10)
C(*i*03)—C(*i*03A)—C(*i*07A)—N(*i*01)	3·4(3)	3·0(3)	−2·5(11)	−2·3(11)
N(*i*02)—N(*i*09)—C(*i*10)—C(*i*11)	−177·6(2)	−179·4(2)	179·4(8)	179·7(7)
N(*i*09)—C(*i*10)—C(*i*11)—C(*i*16)	−6·6(4)	−11·6(4)	16·3(13)	10·4(13)
C(*i*10)—C(*i*11)—C(*i*12)—N(*i*17)	−0·9(4)	1·5(4)	−6·2(11)	−1·6(11)
C(*i*13)—C(*i*12)—N(*i*17)—P(*i*18)	23·1(5)	6·0(4)	−4·2(13)	−10·8(13)
C(*i*12)—N(*i*17)—P(*i*18)—C(*i*19)	176·3(3)	172·2(2)	176·6(7)	177·6(8)
C(*i*12)—N(*i*17)—P(*i*18)—C(*i*25)	60·0(3)	53·0(3)	60·5(8)	61·5(9)
C(*i*12)—N(*i*17)—P(*i*18)—C(*i*31)	−66·6(3)	−70·4(3)	−64·5(8)	−65·2(9)

[a] Molecule (*i*).

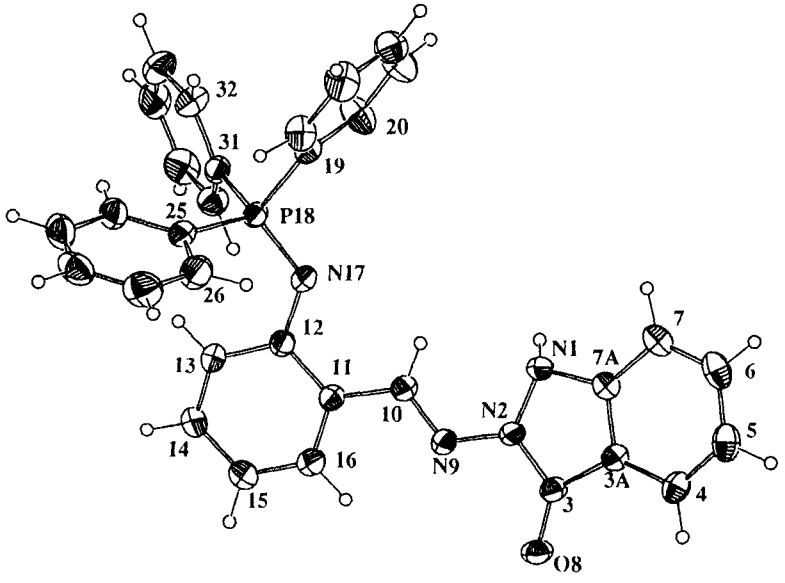

Figure 1. Molecular structure[15] with the numbering system adopted in the crystallographic work. Only one independent molecule (2) of compound **3** is shown for clarity purposes. Thermal ellipsoids for the non-hydrogen atoms are depicted at 30% probability level while hydrogen atoms are represented by spheres (radius = 0·1 Å)

related by a 2_1 axis at 0·2478, 0·0271, z) have essentially the same geometry but differ from that of **3** in the twist of the phenyl rings and to a lesser extent in the conformation of the *ortho* substituents of the benzene ring. This ring is less planar in **3** than in **3**·EtOH [$\Sigma(\Delta/\sigma)^2 = 57{\cdot}95$, 51·62 and 18·95, 6·44 versus the theoretical value of 7·81] and the C(*i*10) and N(*i*17) deviate slightly from this plane in opposite ways to avoid the strain caused by the contact between them [N···C: 2·753(3), 2·833(4) and 2·737(11), 2·707(11) Å in **3** and **3**·EtOH, respectively]. Moreover, examination of the substituent angles (Table 2) shows that the C(*i*10)—C(*i*11) and C(*i*12)–N(*i*17) bonds are bent inwards except the first bond of molecule 2 in **3**. This deformation may be due to the C(*i*10)—H(*i*10)···N(*i*17) intramolecular interactions in spite of the unfavourable geometrical situation of the H(*i*10) with respect to the nitrogen lone pair (Table 3).

All molecules display an *E* configuration around the N(*i*09)=C(*i*10) double bond. The shortening (N_{sp^2}—C_{ar}, C_{ar}—C_{sp^2}, N_{sp^2}—N_{sp^2}) and the elongation (P—N_{sp^2} and, to a certain extent, of C_{sp^2}—N_{sp^2} in **3**·EtOH) of these bonds, with respect to the tabulated values from X-ray and neutron data,[21] is observed as a consequence of some degree of delocalization in the P—N_{sp^2}—C_{ar}—C_{ar}—C_{sp^2}—N_{sp^2}—N_{sp^2} moiety. This fact, together with the previously mentioned intramolecular contact and that of C(*i*16)—H(*i*16)···N(*i*09) (Table 3) could be responsible for the planarity of the molecules (phenyl rings at P excluded). The conformation about the P=N bond corresponds to the parallel one,[22] the C(*i*19) atom being placed *trans* to the C(*i*12) atom.

The bond angles at N(*i*01) indicate an sp^3 hybridization, the angles around it adding 328(3), 328(3) and 338(7), 326(14)° respectively. This tetrahedral situation was previously observed in 2-acetylindazolone [320(2)°][23] (the only reported indazolone in the Cambridge Structural Database),[24] while a less tetrahedral arrangement is displayed by indazolone itself [353(3)°].[10]

The five-membered rings are not planar [$\Sigma(\Delta/\sigma)^2 = 486{\cdot}51$, 1170·80 and 35·07, 53·62 versus the tabulated value of 5·99], adopting a slightly distorted envelope conformation, flapping at N(101) and a twist conformation at N(201), N(202) (compounds **3** and **3**·EtOH) (see Table 2). The ethanol molecules are not significantly different, in terms of the precision achieved, and both have the *trans* conformation [−152(9), −157°].[2]

The packing in the two structures, mainly dominated by hydrogen bonds, is illustrated in Figures 2 and 3. The geometries of the hydrogen interactions are given in Table 3. In compound **3**, each independent molecule (1 and 2) links itself through an intermolecular N—H···O=C bond into infinite chains along the (1/2, y, 1/4) and (0, y, 1/4) two-fold screw axis, respectively. One of these chains, that corresponding to molecule 2, is depicted in Figure 4. Thus, the crystal is built by alternating layers of these chains parallel to the c axis

Table 3. Hydrogen interactions[a]

Compound	X—H···Y	Interatomic distances (Å) X—H	X···Y	H···Y	X—H···Y (°)
3	N(101)—H(101)···O(108)$_1$	0·92(3)	2·799(3)	1·89(3)	170(2)
	N(201)—H(201)···O(208)$_2$	0·89	2·754(3)	1·87(3)	171(4)
	C(110)—H(110)···N(117)	0·93(3)	2·753(3)	2·36(3)	105(2)
	C(210)—H(210)···N(217)	0·95(3)	2·833(4)	2·53(3)	99(2)
	C(116)—H(116)···N(109)	0·97(3)	2·884(3)	2·58(3)	98(2)
	C(216)—H(216)···N(209)	0·97(4)	2·765(4)	2·42(3)	100(2)
	C(234)—H(234)···C1(1–7A)$_3$	1·04(4)	3·581(3)	2·75(5)	137(4)
	C(220)—H(220)···C2(3A–7A)$_2$	1·03(3)	3·518(3)	2·59(4)	150(3)
	C(135)—H(135)···C2(11–16)$_4$	0·98(3)	3·663(3)	2·81(4)	147(4)
1: $1-x,\frac{1}{2}+y,\frac{1}{2}-z$. 2: $-x,\frac{1}{2}+y,\frac{1}{2}-z$. 3: $x,1+y,z$. 4: $x,\frac{1}{2}-y,-\frac{1}{2}+z$.					
3·EtOH	O(250)—H(250)···O(108)	1·02(–)	2·697(10)	1·68(–)	180(–)
	N(101)—H(101)···O(150)	1·12(10)	2·868(9)	1·79(9)	160(8)
	O(150)—H(150)···O(208)	1·00(14)	2·711(10)	1·86(14)	140(11)
	N(201)—H(201)···O(250)$_1$	0·84(14)	2·864(11)	2·03(14)	168(12)
	C(110)—H(110)···N(117)	1·11(9)	2·737(11)	2·40(9)	95(5)
	C(210)—H(210)···N(217)	1·10(11)	2·707(11)	2·40(9)	94(5)
	C(116)—H(116)···N(109)	1·01(10)	2·876(11)	2·39(10)	108(7)
	C(216)—H(216)···N(209)	1·04(7)	2·863(11)	2·43(7)	104(5)
	C(204)—H(204)···C1(11–16)	1·08(8)	3·610(11)	2·58(8)	159(6)
	C(223)—H(223)···C1(11–16)$_2$	1·02(12)	3·441(12)	2·61(12)	139(9)
	C(236)—H(236)···C1(25–30)$_3$	1·03(11)	3·615(11)	2·75(10)	141(8)
	C(104)—H(104)···C2(11–16)$_4$	0·91(8)	3·573(11)	2·73(8)	154(6)
	C(123)—H(123)···C2(11–16)$_5$	0·98(9)	3·506(12)	2·62(9)	151(7)
1: $x,y,z-1$. 2: $x,y-1,z-1$. 3: $x,y-1,z$. 4: $x,y,z+1$. 5: $x,y+1,z$.					

[a] Numbers stand for symmetry operations and *Ci*(1–7A), *Ci*(3A–7A), *Ci*(11–16) and *Ci*(25–30) ($i = 1, 2$) for the centroids of the corresponding rings. (–) Stands for fixed hydrogen atoms.

(Figure 2). In compound **3**·EtOH, the ethanol and the host molecules in the asymmetric unit are connected alternately by O—H···O=C and N—H···O—H hydrogen bonds to construct a ribbon-like structure along the *c* axis. The independent unit of this strand is shown in Figure 5. In addition, quasi 'T' contacts,[25] involving C—H and the five and the six-membered rings, are also present (Table 3).

After performing a smoothing of the van der Waals surface[8] of the free host **3**, by rolling a sphere of radius 1·4 Å,[9] a cavity of volume 12·38 Å^3 (and its symmetry related) almost spherical in shape was located. Its centroid, situated at (–0·0049, –0·0061, 0·3600), led to the following shortest distances 2·52, 2·75, 2·55 and 2·99 Å, H(210),* H(201),* H(224)† and H(227)† being the atoms involved.

A similar study was carried out for **3**·EtOH, excluding the guest molecule. The two independent ethanol molecules were allocated in different types of cages: the molecule labelled as 2 and its centrosymmetrically related are included in a cavity of volume 222·59 Å^3 and of approximately dimensions ±6·33, ±3·83, ±2·88 Å; a section of it through $y = 0·50$ is represented in Figure 6. Molecule 1 is included in a cage of volume and dimensions of 89·49 Å^3 and ±3·81, ±2·63, ±2·53 Å, respectively. For the ethanol molecules, the corresponding volumes, sizes and local packing coefficients, as defined as $C_k = V_{guest}/V_{hole}$, are 51·46 Å^3, ±3·20, ±2·18, +2·01 Å and 0·46 for molecule 2, and 52·55 Å^3, ±3·12, ±2·35, ±2·17 Å and 0·59 for molecule 1.

The structures of **3**·MeOH and **3**·PrOH have not been determined. Although it is obvious that methanol can be accommodated in the hole left by the ethanol molecule, the case of propan-1-ol has to be considered. To determine the volume and size of this molecule, a search in the CSD (July 1991 version, 90 296 entries)[24] was carried out for structures including propan-1-ol as solvate. Only five examples were found which fulfil the following conditions: (i) no disorder present; (ii) crystallographic *R* factor less than 0·10; (iii) no metal atoms present in the structure; (iv) fractional coordinates available. Of these five, only one (CSD refcode ESTRPD)[26] has the hydrogen atoms of the propanol

* $-x, -1/2+y, 1/2-z$.
† $x, 1/2-y, 1/2+z$.

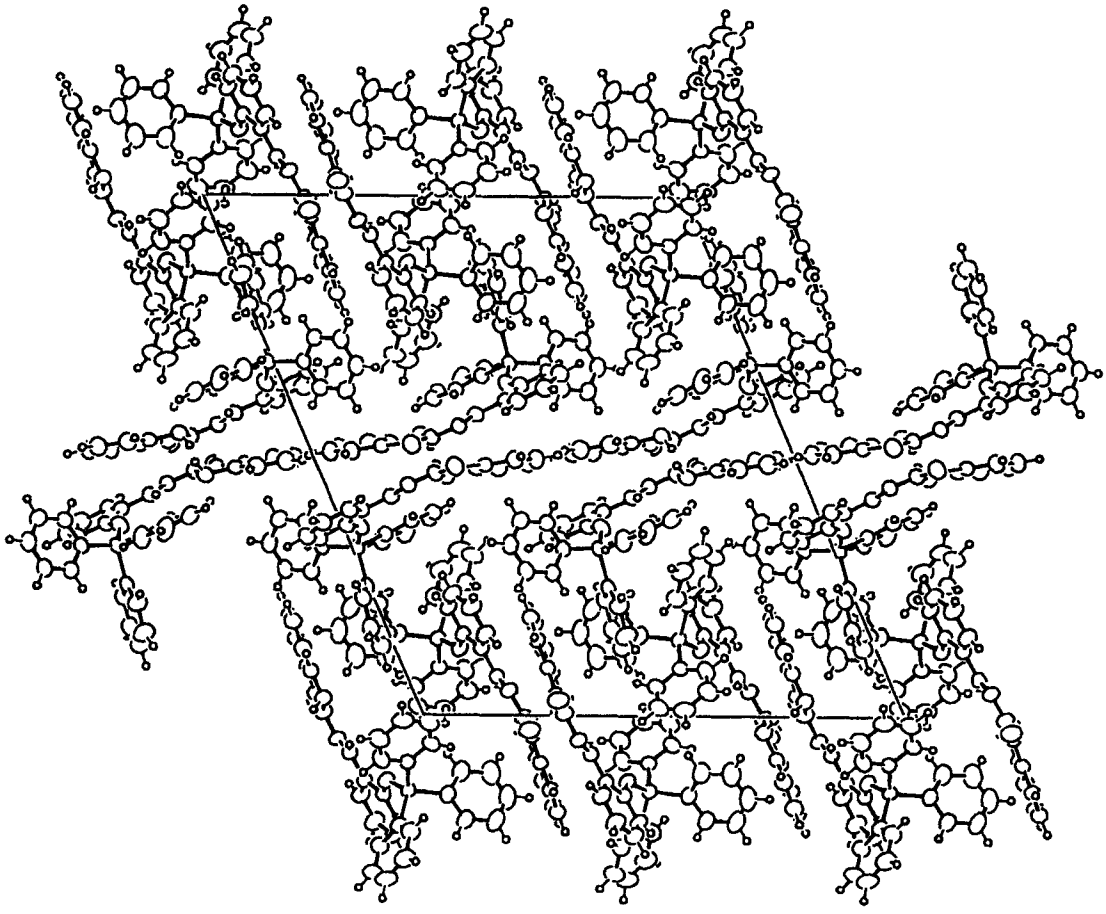

Figure 2. Compound 3: a view of the packing along the *b* axis (Ellipsoids at 30%)

molecule located, which are necessary to use the program HOLES: it contains a propan-1-ol molecule in the '*gauche*' conformation (O—C—C—C = −65·4°). The model of interpenetrating spheres of van der Waals radii[8,9] gives values of 66·62 Å^3 and ±3·27, ±2·56 and ±2·35 Å for volume and size, respectively. Therefore, if the smallest hole of molecule 1 (**3**·EtOH, 89·49 Å^3) is considered, the propan-1-ol molecule can be included in the same host matrix displaying a local packing coefficient $C_k = 0{\cdot}74$, higher than those above reported for the ethanol case but similar to those found by us for the BF_4^- anion where the fluorine atoms are involved in hydrogen interactions.[27,28]

The ^{13}C NMR spectra of the free host **3** and those of its three alcohol inclusion derivatives were recorded in the solid state using the CP/MAS technique. The chemical shifts are given in Table 4, which also includes the data in solution (see Experimental).

Concerning the chemical shifts of the host, the three inclusion compounds present very similar values; as a consequence, those in Table 4 are averaged values. The only noticeable difference is that the resolution of the spectrum increases regularly from **3** (the worst) to **3**·PrOH (the best). The differences between the chemical shifts of the host in DMSO-d_6 solution and the pure host in the solid state ($\Delta\delta = \delta_{soln} - \delta_{solid}$) and those, in the solid state, between the pure host and the inclusion compounds ($\Delta\delta' = \delta_{solid} - \delta_{HG}$) are also reported in Table 4.

The largest $\Delta\delta$ values, about 3·3 ppm, are observed for C-9 and C-12. Probably, the conformation about the N—C-9 bond changes between the solid state and the solution. The fact that the highly polarized iminophosphorane[22] is more or less conjugated with the phenyl ring should affect mainly the *ipso* (C-9) and the *para* (C-12) carbon signals.

Concerning $\Delta\delta'$, the largest values correspond to C-3a and C-4. We assign these shifts to the hydrogen

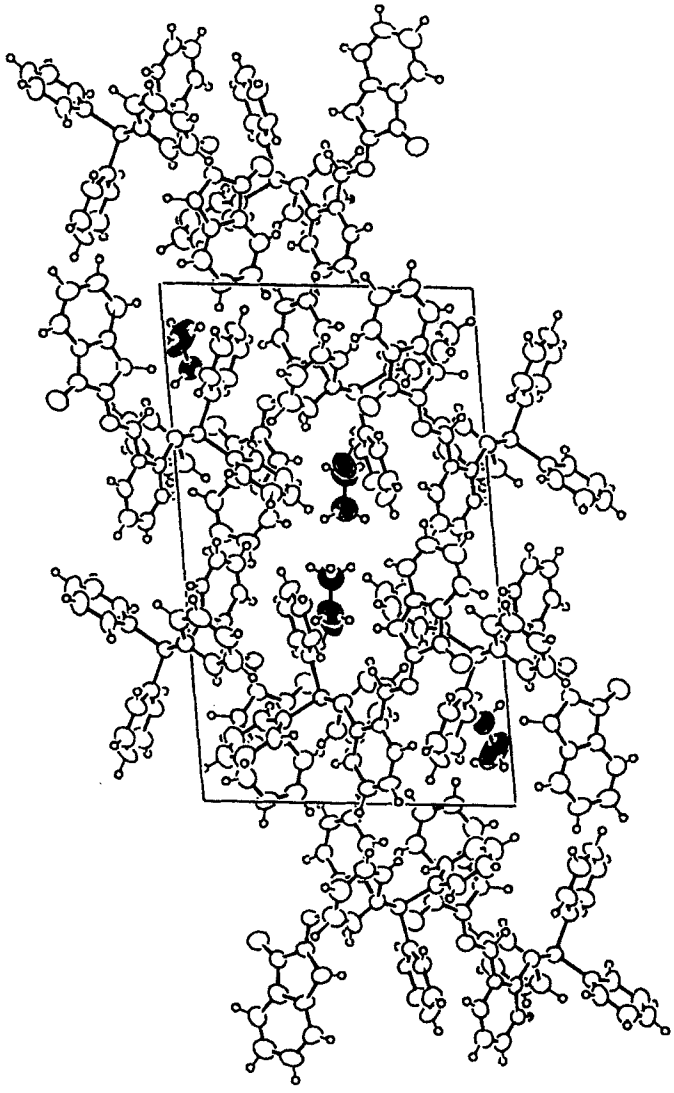

Figure 3. Same as Figure 2 for compound **3**·EtOH. (Ellipsoids at 30%)

bond between the OH of the alcohol and the carbonyl group of the indazolone. Contrary to naive expectations, it is not C-3 but the adjacent atoms which are the most sensitive carbons in indazolones.[10]

The signals of the guest are clearly observed. The CP/MAS technique allows one to identify the guest and to determine the host–guest stoichiometry in a non-destructive way. The signals appear (with the differences with respect to the values in solution reported under Experimental in parentheses) as follows: methanol at 49·08 ppm (−1·5 ppm), ethanol at 18·06, CH_3 (−0·2 ppm), 56·11 ppm, CH_2 (−2·1 pm); propan-1-ol at 11·27, CH_3 (1·2 ppm), 26·11 ppm, central CH_2 (0·4 ppm) and 63·33 ppm, CH_2OH (−1·1 ppm). The effect on the terminal CH_3 in propanol is probably due to the proximity of a phenyl ring in the crystal, whereas the systematic deshielding of the carbon linked to the OH is attributable the hydrogen bonds present in the crystal (see the structural discussion of **3**·EtOH):

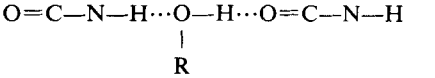

The ^{13}C NMR spectra of propanol in $CDCl_3$ without and with one equivalent of pyridine (as an HB acceptor)

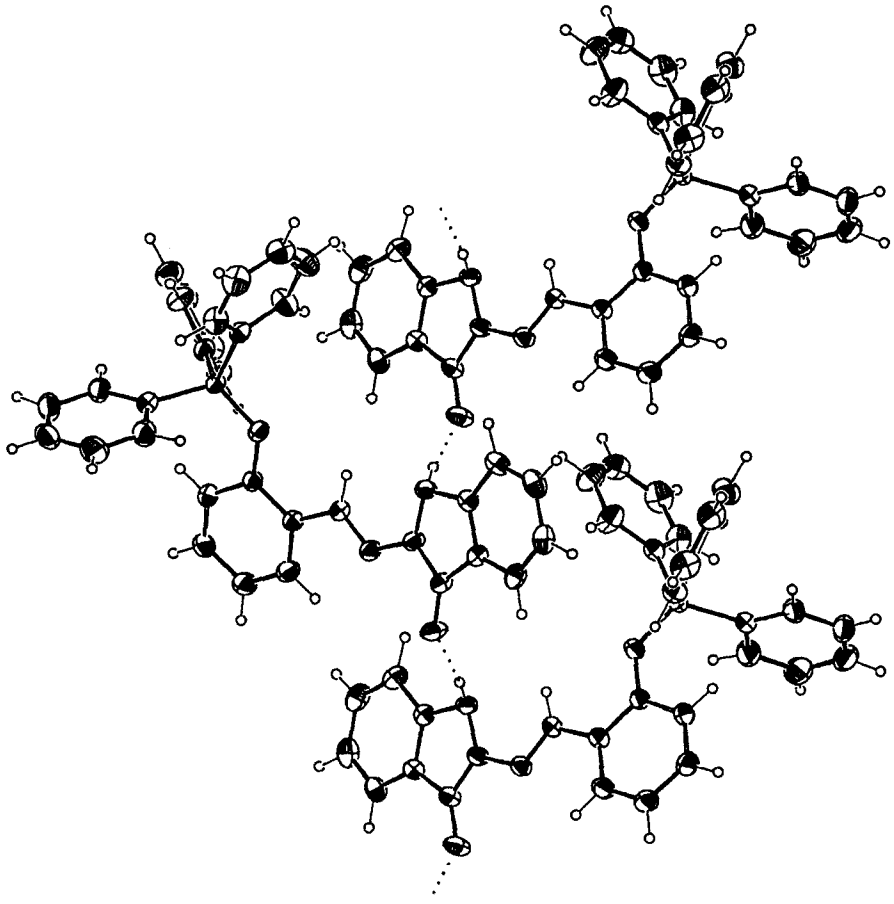

Figure 4. Compound **3**: perspective of one chain showing the hydrogen bond interactions. (Ellipsoids at 30%)

Table 4. Carbon-13 chemical shifts (ppm) and chemical shifts differences (ppm) of the host **3** in different situations

Carbon	Solution	Pure host	Host–guest	$\Delta\delta = \delta_{soln} - \delta_{solid}$	$\Delta\delta' = \delta_{solid} - \delta_{HG}$
C-3	159·12	158·10	158·19	1·02	−0·09
C-3a	119·36	119·17	119·97	0·19	−0·80
C-4	124·16	125·23	124·09	−1·07	1·14
C-5	122·40	123·64	123·19	−1·24	0·45
C-6	132·45	131·84	131·95	0·61	−0·11
C-7	113·04	112·87	112·88	0·17	−0·01
C-7a	145·76	146·27	146·49	−0·51	−0·22
C-H	145·85	146·27	146·49	−0·42	−0·22
C-8	127·96	127·27	127·91	0·59	−0·64
C-9	155·55	152·38	152·81	3·17	−0·43
C-10	123·08	123·64	123·19	−0·56	0·45
C-11	130·60	129·55	130·20	1·05	−0·65
C-12	118·74	115·29	115·91	3·45	−0·62
C-13	127·31	127·27	127·91	0·04	−0·64
C-14	129·79	130·05	129·07	0·24	0·48
C-15	132·55	132·71	131·95	−0·16	0·76
C-16	128·70	127·27	127·91	1·43	−0·64
C-17	132·02	131·84	131·94	0·18	−0·10

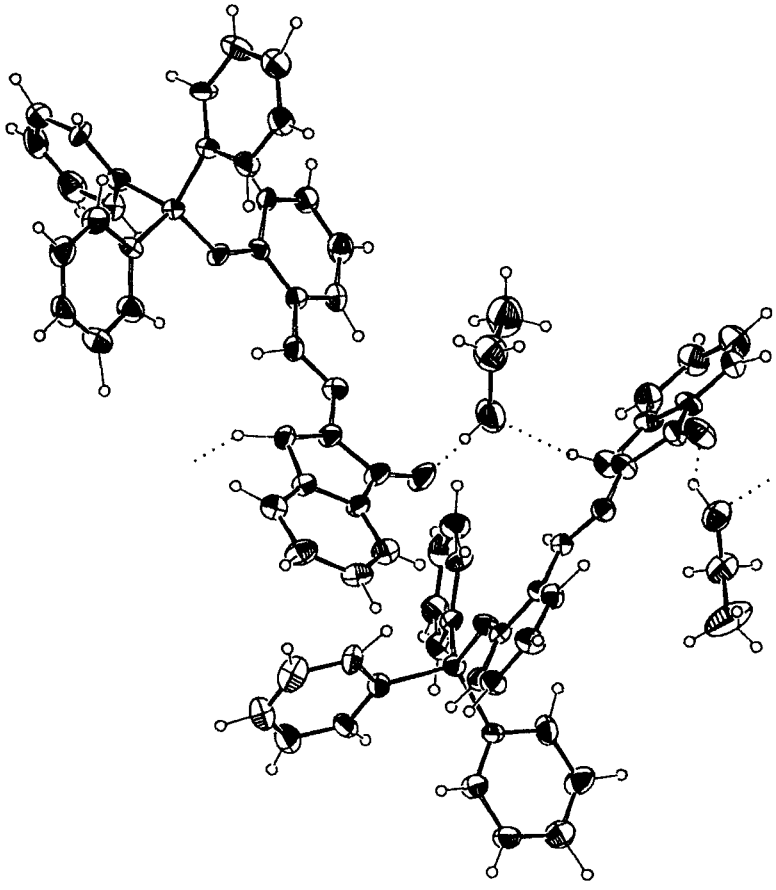

Figure 5. Same as Figure 4 for compound **3**·EtOH. (Ellipsoids at 30%)

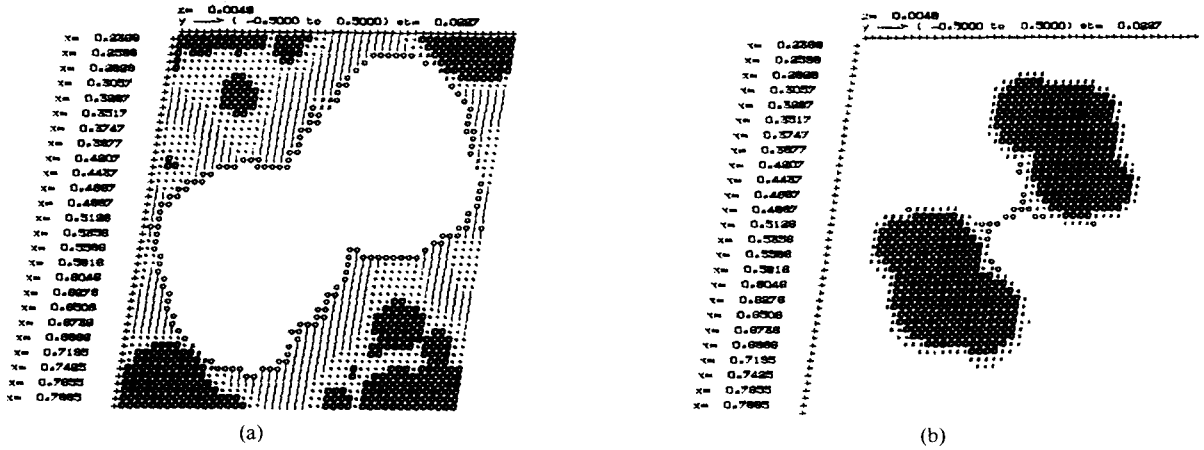

(a) (b)

Figure 6. Section[9] $y = 0{\cdot}50$ showing the hole (a) where the two ethanol molecules (2) centrosymmetrically related are included and (b) the same section for the ethanol molecules (2)

and with one equivalent of trifluoroacetic acid (as an HB donor) were recorded. The trifluoroacetic acid does not shift the terminal CH_2 signal, but pyridine produces an effect similar in sign to but smaller ($-0{\cdot}42$ ppm instead of $-1{\cdot}1$ ppm) than that observed in **3**·PrOH compared with **3**. The effect is larger in the solid state because all propanol molecules are hydrogen bonded whereas in solution there is an equilibrium between hydrogen-bonded and free propanol molecules.

CONCLUSIONS

The combined use of three methods, X-ray crystallography, thermal analysis and solid-state NMR, is necessary to understand the properties of inclusion compounds. Crystallography yields the most valuable information but it suffers from two drawbacks: it is too time consuming for a systematic survey and in some cases good crystals cannot be obtained. Thermal analysis gives a macroscopic view of the energies involved in the host–guest interaction. Solid-state NMR (in most cases ^{13}C NMR) gives a picture of the molecular interactions, hydrogen bonds and proximity effects. In the present case, the X-ray structures of **3** and **3**·EtOH have been determined. On this basis, the DSC and ^{13}C NMR chemical shifts can be interpreted. Further, they predict that the two other inclusion compounds, **3**·MeOH and **3**·PrOH, should be similar to the ethanol derivative (i) in the structure of the host, (ii) in the size of the cavity and (iii) in the hydrogen-bond networks that link the guest in the cavity of the host.

SUPPLEMENTARY MATERIAL

Tables of atomic coordinates, anisotropic displacement parameters for the non-hydrogen atoms and structure factors can be obtained from the authors on request.

ACKNOWLEDGEMENTS

Financial support was provided by the Dirección General de Investigación Científica y Técnica (PB87-0291).

REFERENCES

1. P. Molina, M. Alajarín, M. J. Pérez de Vega, C. Foces-Foces, F. H. Cano, R. M. Claramunt and J. Elguero, *J. Chem. Soc., Perkin Trans. 2* 1853–1860 (1987).
2. C. Foces-Foces, F. H. Cano, P. Molina, M. Alajarín, M. J. Pérez de Vega, J. Palazón, R. M. Claramunt and J. Elguero, *Tetrahedron*, **44**, 5117–5130 (1988).
3. F. Todd, K. Tanaka, J. Elguero, L. Nassimbeni and M. Niven, *Chem. Lett.* 2317–2320 (1987).
4. F. Todd, K. Tanaka, J. Elguero, Z. Stein and I. Goldberg, *Chem. Lett.* 1061–1064 (1988).
5. A. L. Llamas-Saiz, C. Foces-Foces, P. Molina, M. Alajarin, A. Vidal, R. M. Claramunt and J. Elguero, *J. Chem. Soc., Perkin Trans. 2* 1025–1031 (1991).
6. E. Weber, C. Wimmer, A. L. Llamas-Saiz and C. Foces-Foces, *J. Chem. Soc., Chem. Commun.* submitted for publication.
7. G. Boyer, R. M. Claramunt, C. Foces-Foces, A. L. Llamas-Saiz and J. Elguero, unpublished results.
8. F. H. Cano and M. Martínez-Ripoll, *J. Mol. Struct.* in press (1992).
9. M. Martínez-Ripoll, F. H. Cano and C. Foces-Foces, *Program HOLES*. To be published.
10. P. Ballesteros, J. Elguero, R. M. Claramunt, R. Faure, C. Foces-Foces, F. H. Cano and A. Rousseau, *J. Chem. Soc., Perkin Trans. 2* 1677–1681 (1986).
11. A.-B. N. Luheshi, S. M. Salem, R. K. Smalley, P. D. Kennewell and R. Westwood, *Tetrahedron Lett.* **31**, 6561–6564 (1990).
12. Y. Nomura, Y. Kikuchi and Y. Takeuchi, *Chem. Lett.* 575–576 (1974).
13. M. C. Burla, M. Camalli, G. Cascarano, C. Giacovazzo, G. Polidori, R. Spagna and D. Viterbo, *J. Appl. Crystallogr.* **22**, 389–393 (1989).
14. J. M. Stewart, P. A. Machin, C. W. Dickinson, H. L. Ammon, H. Heck and H. Flak, *The X-Ray System*, Technical Report TR-446. Computer Science Center, University of Maryland (1976).
15. S. R. Hall and J. M. Stewart, *Xtal3.0*. Universities of Western Australia, Perth and Maryland, USA (1990).
16. M. Martínez-Ripoll and F. H. Cano, *PESOS*, unpublished program.
17. N. Walker and D. Stuart, *Acta Crystallogr., Sect. A* **39**, 158–166 (1983).
18. *International Tables for X-Ray Crystallography*, Vol. IV. Kynoch Press, Birmingham (1974).
19. R. C. Weast (Ed.), *CRC Handbook of Chemistry and Physics*, 65th ed., p. C-694. CRC Press, Boca Raton, FL (1984).
20. N. G. Parsonage and L. A. K. Staveley, in *Inclusion Compounds*, edited by J. L. Atwood, J. E. D. Davies and D. D. MacNicol, Vol. 3, p. 1. Academic Press, London (1984).
21. F. H. Allen, O. Kennard, D. G. Watson, L. Brammer, A. G. Orpen and R. Taylor, *J. Chem. Soc., Perkin Trans. 2* 1–19 (1987).
22. P. Molina, M. Alajarín, C. L. Leonardo, R. M. Claramunt, C. Foces-Foces, F. H. Cano, J. Catalán, J. L. G. de Paz and J. Elguero, *J. Am. Chem. Soc.* **111**, 355–363 (1989).
23. D. L. Smith and E. K. Barret, *Acta Crystallogr, Sect. B* **25**, 2355–2361 (1969).
24. F. H. Allen, O. Kennard and R. Taylor, *Acc. Chem. Res.* **16**, 146–53 (1983).
25. G. R. Desiraju, *Crystal Engineering*. Elsevier, Amsterdam (1989).
26. B. Busetta, C Courseille, S. Geoffre and M. Hospital, *Acta Crystallogr., Sect. B 28*, 1349–1351 (1972).
27. A. L. Llamas-Saiz, C. Foces-Foces, J. Elguero, P. Molina, M. Alajarín and A. Vidal, *J. Chem. Soc., Perkin Trans. 2* 1667–1676 (1991).
28. A. L. Llamas-Saiz, C. Foces-Foces, J. Elguero, P. Molina, M. Alajarín and A. Vidal, *J. Chem. Soc., Perkin Trans. 2* 2033–2040 (1991).